SOURCE MECHANISMS FOR EXPLOSIONS IN BARRE GRANITE

Anastasia Stroujkova[1], Jessie L. Bonner[1], Xiaoning Yang[2], Brian W. Stump[3], and William R. Walter[4]

Weston Geophysical Corporation[1], Los Alamos National Laboratory[2], Southern Methodist University[3], and Lawrence Livermore National Laboratory[4]

Sponsored by the National Nuclear Security Administration

Contract Nos. DE-AC52-08NA28655[1,3], LA08-BAA08-97-NDD03[2], and LL08-BAA08-97-NDD03[4]
Proposal No. BAA08-97

ABSTRACT

The previously conducted Arizona Source Phenomenology Experiments (SPE) and the Non-Proliferation Experiment (NPE) represent two unique datasets that could provide critical information about the partitioning of important regional phases, such as *P*, *S*, and *Lg*, from explosions. A new explosion experiment named the New England Damage Experiment (NEDE) was conducted in July 2008 in a granite quarry near Barre, VT. Five explosions with various types of explosives with different Velocities Of Detonation (VOD) have been detonated: low VOD (black powder, Shot 1); medium VOD (ANFO+emulsion, Shots 2 and 4); and fast VOD (COMP B, Shots 3 and 5). The yields for these five single-fired blasts ranged from 134 to 270 lbs of explosives. The main objective of the experiment was an *in situ* study of the influence of VOD on resulting amount of damage and failure modes.

An important part of this project is to compare the moment tensors from these explosions with other data from different media and confining conditions. The moment tensor inversion was performed using the methodology developed in Stump and Johnson (1977). The inversion code was written by David Yang (Yang, 1997). To compute the Green's functions required for the inversion we developed a 1D velocity model of the testing area using the laboratory measurements and the seismic refraction data. The Green's functions were computed using the wavenumber integration technique (Herrmann, 2002). We used five near-source stations to reconstruct moment tensors for each explosion, as well as their time histories. The solutions have the dominant diagonal elements; however some explosions have significant off-diagonal components. The horizontal diagonal components (M_{xx} and M_{yy}) are similar in size, while the vertical M_{zz} is approximately twice as large as each of the horizontals. The size of the isotropic component varies between 72% and 79% for different shots and doesn't appear to correlate with the type of the explosives used in our experiments. The moment tensors from the previous experiments conducted in granites (Morenci copper mine) are consistent with the results obtained in Barre granites.

OBJECTIVES

Recent advances in explosion source theory indicate that the damage that occurs near an explosion is a prominent source of *S*-wave energy. The Ashby and Sammis (1990) model for crack nucleation and growth predicts *S*-wave generation in the far field (Sammis, 2002). The moment tensor information is important for understanding issues related to shear wave generation mechanism(s) and other aspects of the source phenomenology. Modeling by Patton et al. (2005) and Stevens et al. (2003a) have shown the importance of the cone of damage above a source, modeled by a compensated linear vector dipole (CLVD), in generating *Rg* in the near field and *S (Lg)* in the far field, respectively. The phenomenology in the CLVD regime includes block motions, crack damage, and spallation.

The Arizona SPE and the NPE represent two unique datasets that could provide important information about the generation from *S*-waves from explosions. A new explosion experiment (NEDE) was conducted in July 2008. An objective of this project is to compare the moment tensors from these explosions with other data from different media and confining conditions.

RESEARCH ACCOMPLISHED

Experiment Summary

Weston Geophysical Corporation, New England Research, Inc., and a variety of blasting consultants conducted the field phase of the New England Damage Experiment (NEDE) in a granite quarry near Barre, VT. The experiment was conducted in July 2008, and further experiment details are given in Leidig et al. (2008). The purposes of this experiment were to investigate: (1) generation of fractures from small explosions in homogenous, relatively un-fractured granite, (2) quantify the near-source, local, and regional distance phase generation from the explosions, and (3) compare and contrast the seismic phase generation to the rock damage. We studied moment tensors of the five explosions that were carried out during this experiment.

The test site is situated in the Siluro-Devonian alkaline pluton injected into sedimentary rocks (Figure 1a), later subjected to a regional metamorphism during Acadian orogeny (e.g., Richter, 1987). The emplacement metasediments belong to Gile Mountain and Waits river formations represented by schists and quartzites. Figure 1b shows the map of the experiment with the test site and the near-source stations shown.

The fine-grained grey Barre granite has been quarried for over 200 years as a monument stone due to its low fracture density and homogeneous composition. While coring the granite for our test applications, the driller often had to snap the core from the bottom of the hole due to a lack of naturally occurring fractures. The upper 50 feet of fractured and weathered granite had been stripped off at this site, which allowed us to be closer in depth to the relatively unfractured, monument-quality Barre granite (see Leidig et al. [2009, these Proceedings] for further information).

Five explosions were detonated at the test site on 12 July 2008 (Table 1). The yields for these five single-fired blasts ranged from 134 to 270 lbs of explosives. Three explosive types with dramatically different VOD were used: black powder (low VOD, Shot 1); ANFO+emulsion (medium VOD, Shots 2 and 4); and COMP B (fast VOD, Shots 3 and 5). The NEDE explosions were recorded on over 140 seismic instruments, including short-period seismometers, high-g accelerometers, and a high-resolution video camera, deployed at distances of less than 5 m to 30 km from the explosions. To compute moment tensors we used only the data from the 3C instruments located closer than 500 m from the stations (e.g., Table 2).

Velocity Model Development

In order to calculate Green's functions at the near-source stations (less than 500 m from the sources) we first needed to develop a velocity model valid for the upper 100 m. To develop the velocity model, we used data from both seismic field and laboratory rock core measurements. The velocities in the upper part of the subsurface down to 60 ft (about 20 m) were measured using cores from several boreholes (Peter Boyd, see acknowledgements) by New England Research (NER). The measurements show a gradual velocity increase from approximately 4.0 km/s at the surface to 4.4 km/s at a depth of approximately 30 meters, where it reaches a plateau (Figure 2a, red triangles).

The velocity below 20 m was found by examining the travel times of the first arrivals. Figure 2b shows the travel times picked manually for the near-source 3C and Texan stations. The picks show considerable scatter due to a heterogeneous near-surface structure, elevation differences, and possibly timing errors for different shots. The apparent velocity estimated by fitting a straight line is V_p = 4.9 km/s. The shear-wave velocity (V_s = 2.72 km/s) was found using a V_p/V_s ratio of 1.8. These velocities, however, describe the average velocity in the first 300–400 m below the surface and it is impossible to pinpoint where the velocity changes from 4.4 km/s to 4.9 km/s. Therefore, for the purpose of constructing the Green's functions, we set the lower layer V_p to 4.5 km/s, which corresponds to the highest velocity measured in the rock samples. The final velocity profile is shown in Figure 3a.

Strong velocity anisotropy has been reported at the site from both rock sample measurements made by NER and seismic travel time studies (e.g., Leidig et al., 2008). The differences between laboratory measured fast and slow velocities are on the order of 10–20 %. Engelder et al. (1977) attributed the anisotropy in Barre granite to the opening of microfractures due to residual stresses. Most of the microfractures' strike azimuths are close to 30º, which is approximately parallel to the rift orientation.

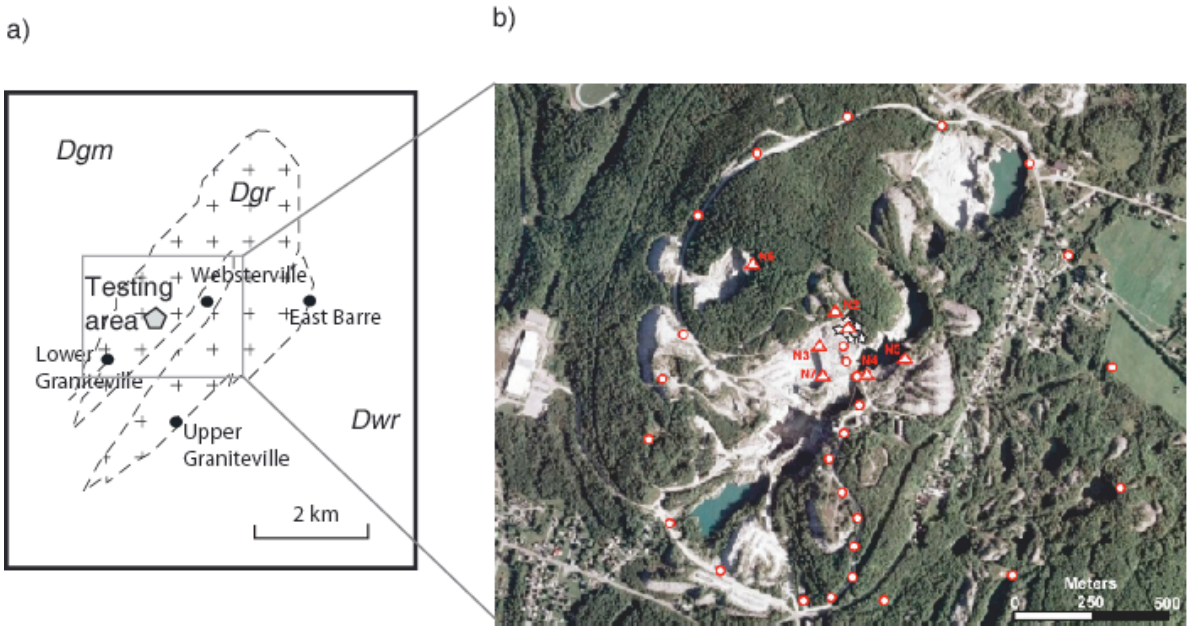

Figure 1. a) The geological map of Barre pluton (from Richter, 1987). The geological formations are: *Dgr* – Devonian granites, *Dgm* – Gile Mountain formation, *Dwr* – Waits river formation. b) The Google Earth picture of the area marked in a bounding box in a). The shots (white stars with black outline) are seen in the middle of the image (the test site). Also shown the near-source 3C stations N1-N7 and Texans NT01-NT27.

Table 1. Origin Characteristics for NEDE Shots.

Shot	Latitude (ºN)	Longitude (ºW)	Elevation (m)	Borehole/ Centroid Depth (m)	Stemming (m)	Yield (lbs)	Explosive
1	44.15774	-72.47848	509	9.1/8.5	7.3	134	Black Powder
2	44.15800	-72.47813	509	11.3/10.7	10.1	135.5	ANFO/Emul 50:50
3	44.15780	-72.47770	503	11.3/10.7	10.4	136	COMP B
4	44.15751	-72.47797	508	13.7/12.8	11.6	269.5	ANFO/Emul 50:50
5	44.15754	-72.47757	503	13.7/12.8	11.9	270	COMP B

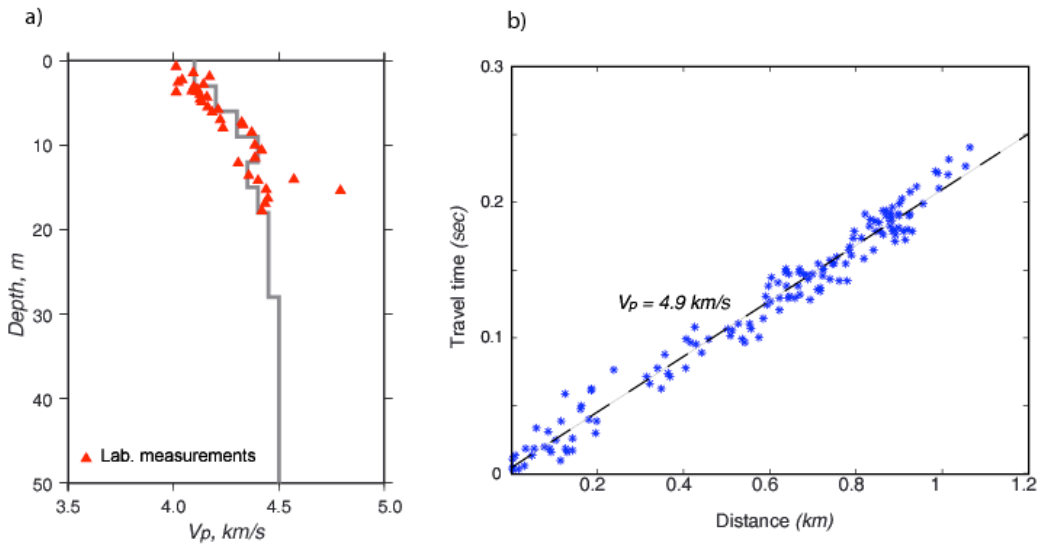

Figure 2. a) Final velocity (V_p) model. Triangles show the velocity measurements made by NER at CH1 site prior to the explosions. b) Travel time picks for the near-source 3C stations and Texans. Dashed line shows the linear least square fit with the slope corresponding to V_p=4.9 km/s.

Table 2. Distances and elevation differences between the shots and the stations.

Shot #	Distance/Elevation difference, *m*				
	N2	N3	N5	N6	N7
1	58.8/24	86.2/-17	238.4/-3	356.7/-20	161.4/-7
2	49.0/24	126.3/-17	227.5/-3	364.0/-20	198.5/-7
3	89.9/30	142.3/-11	186.6/3	404.8/-14	196.0/-1
4	98.6/25	110.8/-16	190.6/-2	404.9/-19	157.4/-6
5	116.2/30	142.4/-11	163.1/3	429.0/-14	180.5/-1

To perform the moment tensor inversion we used five 3C stations (N2, N3, N5, N6 and N7) located at distances between 58 m and 429 m from the explosions (Table 2). Figure 3 shows comparison between the vertical components of the data and the explosion Green's functions (*ZEX*). There are significant discrepancies between the data and the Green's function amplitudes, especially for the stations located further away from the test site (Stations N5-N7). The synthetic *Rg* amplitudes are significantly larger than the measured amplitudes. Since the large signal in the synthetics is produced by the free-surface interaction, it depends on the shot depth, source excitation, roughness of the free surface (surface wave scattering) and the attenuation of the upper layer. This discrepancy was noted in Yang and Bonner (2009), where the authors proposed to adjust the shot depths in order to reduce *Rg* amplitudes. In this experiment, the stations with large discrepancies are located at about the same depth or lower then the datum for the explosion boreholes (Table 2, Leidig et al., 2008). Therefore the depth adjustments would not be helpful in this case.

Figure 4a shows peak amplitudes of *Rg* measured using the data from the Texans located between 0.6 and 1.2 km. To correct for the geometric spreading, the amplitudes were multiplied by a square root of distance. The amplitudes show systematic decrease for azimuths from about 60º through 210º. One explanation is a scattering of *Rg* by topographic features: there is a deep trough from previous excavations extending from NE toward SW. The depth of the water-filled pit near stations N4 and N5 could reach 90 m (Leidig et al., 2008). The amplitude decrease could also be caused by a lithological change from the granites to the emplacement rocks of Gile Mtn. formation (schists). The lithology change could be inferred from the geological map (Figure 1a) from Richter (1987).

Figure 4b shows the waveform data from the Texan stations located between 600m and 1000m from the explosions. The waveforms are corrected for the geometric spreading and plotted as a function of the station azimuths. The

decrease in *P*-wave amplitudes in the azimuth range between 60º and 210º (Figure 4b) also supports the idea that the amplitude decay is due to a lithology change, since *P*-wave amplitudes are less sensitive to the topographic scattering. This figure demonstrates that there is a strong propagation-induced azimuthal pattern, which can potentially influence the moment tensors. In order to minimize the propagation effects, we only used the stations located within 500 m from the explosions.

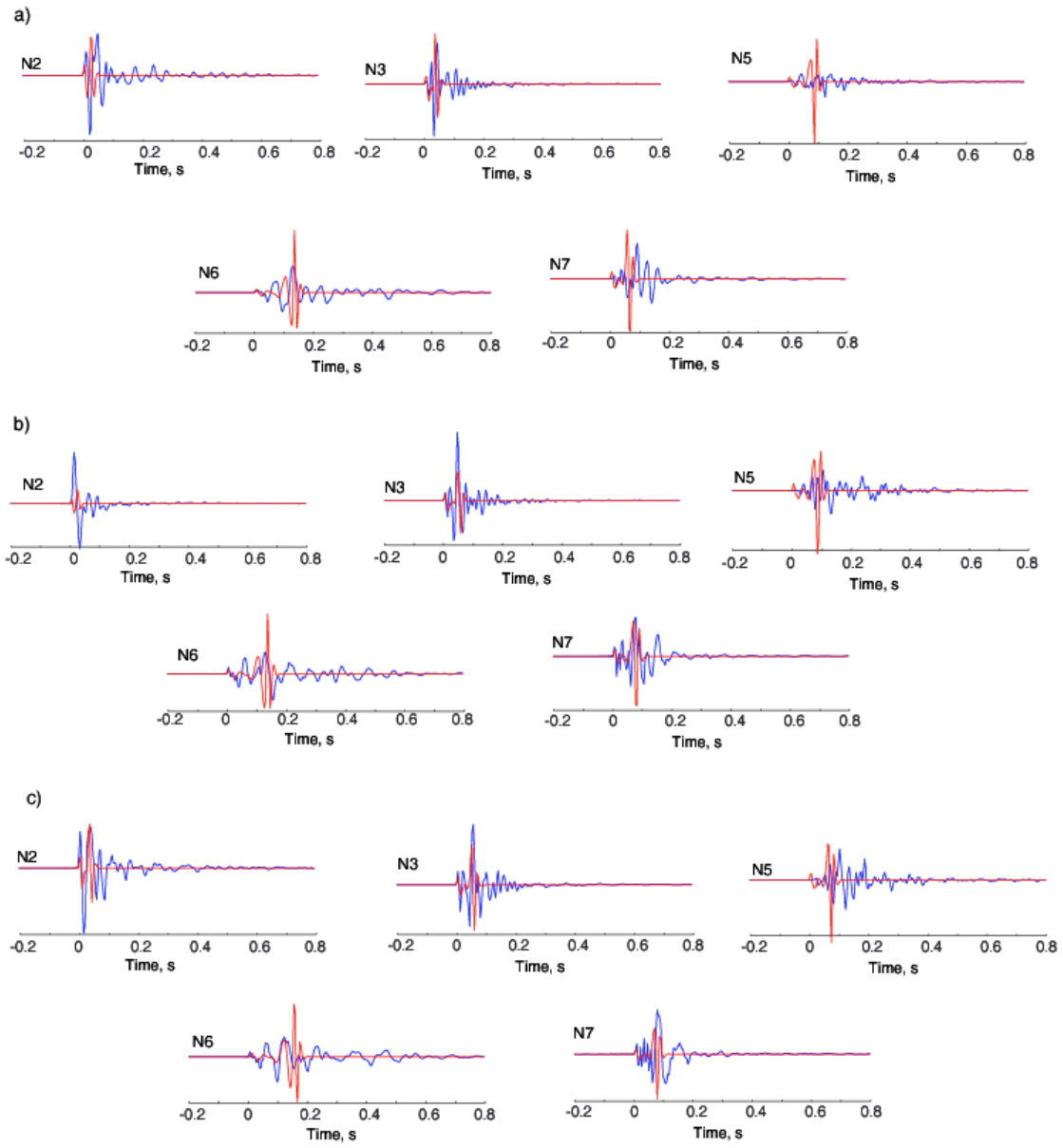

Figure 3. Comparison between the data (blue) and the Green's functions (red). Traces are scaled to maintain the same ratio between the data and the Green's function amplitudes. a) Shot 1; b) Shot 2; c) Shot 3; d) Shot 4; e) Shot 5.

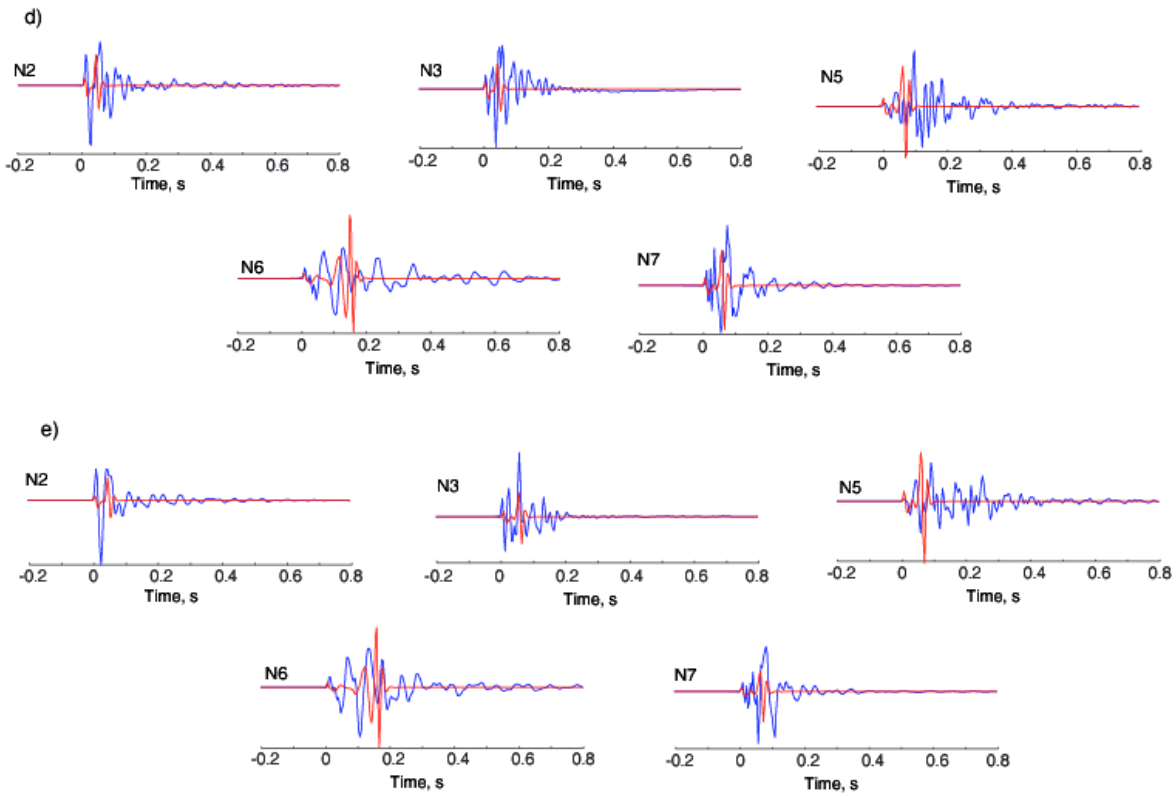

Figure 3. ***Continued.***

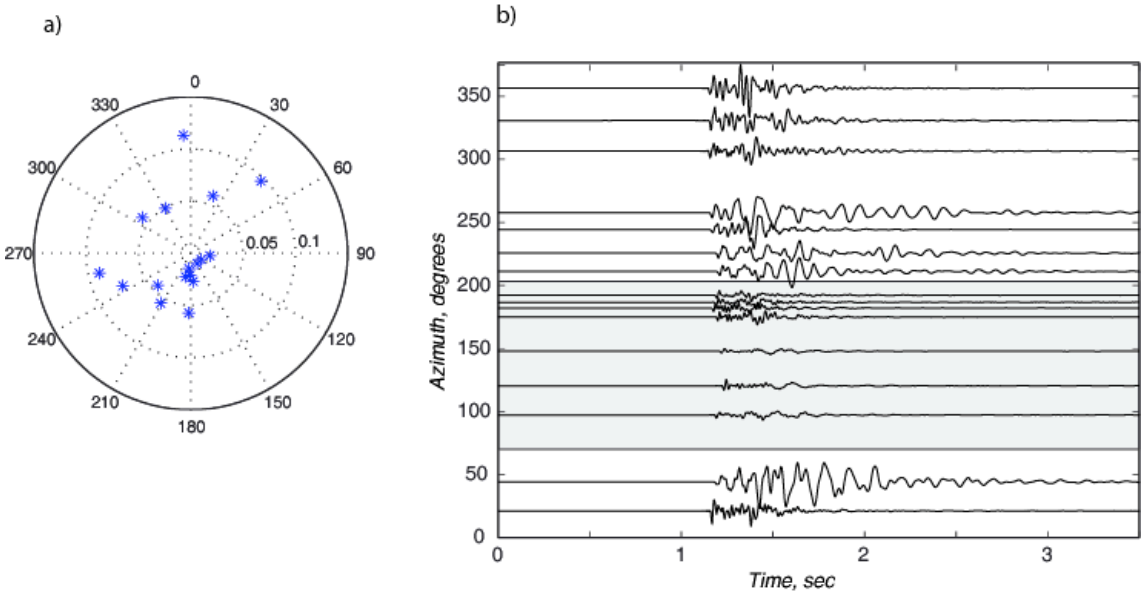

Figure 4. a) A polar plot of *Rg* peak amplitudes multiplied by a square root of distance for Shot 5. The amplitudes are from the near-source Texans. b) The waveforms from Shot 5 recorded at the near-source Texans. The amplitudes are corrected for the geometrical spreading. The shaded area shows the azimuth range where the significant amplitude decrease is observed.

Inversion Results

The moment tensor inversion was performed using the methodology developed in Stump and Johnson (1977) using the inversion code written by David Yang (1997). The inversion is performed in the frequency domain by solving a system of linear equations (Stump and Johnson, 1977):

$$d_i = G_{ij,k} m_{jk} \tag{1}$$

where d_i are the measured ground velocities, $G_{ij,k}$ are the Green's functions for ground velocities, and m_{jk} are the components of the moment tensor to be determined. The inversion is repeated for each frequency, and then transformed back into the time domain to produce moment tensor time histories. The solution of the linear system (1) is performed using singular value decomposition (SVD). The Green's functions $G_{ij,k}$ are calculated using *CPIS3.30* software package (e.g., Herrmann, 2002).

The first step in data preprocessing included the application of the instrument corrections and re-sampling to 250 samples per second. Then, the observed traces were manually aligned with the Green's functions. The inversion produced both high-frequency and low-frequency artifacts in the time-dependent moment-rate tensor components. According to Yang (1997) the high-frequency noise is due to imperfect (manual) alignment of the data and the Green's functions. The low-frequency artifacts are due to differences between the model and actual medium (Green's function discrepancies). To minimize the effect of the artifacts the time-domain moment tensors were bandpass-filtered between 8 Hz and 50 Hz.

To analyze the moment tensor solutions we calculated the percentages of the isotropic component using the relationship (Feignier and Young, 1992):

$$R = \frac{tr(M) \times 100\%}{|tr(M)| + \sum |m_i|} \tag{2}$$

where M is the moment tensor, and m_i are the deviatoric eigenvalues. For a purely isotropic source $R = 100\%$. The percentages can be calculated for each time slice of the moment tensor. To assign the percentage of an isotropic component for each explosion we found R for the time slice where the value $|tr(M)|$ reaches its maximum.

The resulting time-dependent moment tensors are shown in Figure 5. The diagonal elements dominate for most explosions. The amplitudes of M_{xx} and M_{yy} components of the moment tensors are similar, while the amplitudes of M_{zz} components exceed the horizontals by almost a factor of 2. This could correspond, for instance, to a combination of a volumetric source and a single force or a CLVD. The percentages of the isotropic component vary between 72% and 79% for different shots. There is no apparent correlation between the explosive type and the moment tensor. For example, Shot 2 (ANFO+emulsion) has the largest isotropic components (79%, Table 3). On the other hand, Shot 4 (also ANFO+emulsion) has the largest off-diagonal and the smallest isotropic components (72%, Table 3). We note that Leidig et al. (2009, these Proceedings) do see differences in the shear waves generated by the different shot types. The relatively high percentage of non-isotropic component could be an artifact of an inadequate velocity model.

Table 3. Moment tensor inversion results

Shot #	M_{xx} $\times 10^{12}$ N×m	M_{xy} $\times 10^{12}$ N×m	M_{xz} $\times 10^{12}$ N×m	M_{yy} $\times 10^{12}$ N×m	M_{yz} $\times 10^{12}$ N×m	M_{zz} $\times 10^{12}$ N×m	% *iso*
1	2.0327	0.0665	-0.0933	2.0270	-0.2380	3.6346	78
2	2.8945	0.0055	-0.7483	2.8456	-0.2131	4.4661	79
3	3.0699	-0.1931	0.1275	3.3284	0.4748	6.1910	75
4	5.3061	-0.2564	1.2209	5.1246	1.4592	10.1972	72
5	4.4442	-0.0915	0.0273	4.7618	0.1109	8.7154	77

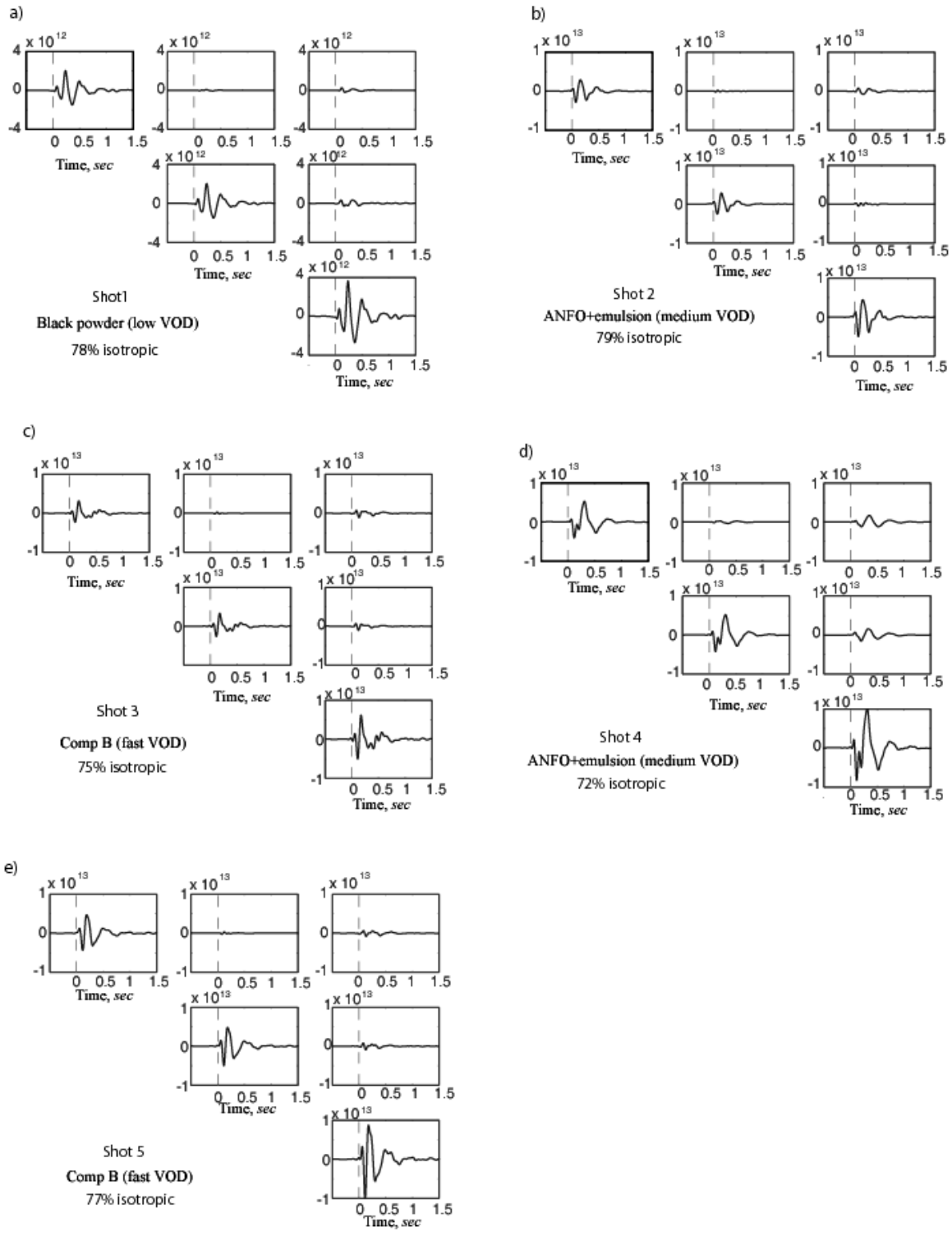

Figure 5. Moment tensor inversion results for: a) Shot 1; b) Shot 2; c) Shot 3; d) Shot 4; and e) Shot 5. Each shot panel shows 6 traces corresponding to 6 moment tensor components (M_{xx}, M_{xy}, M_{xz}, M_{yy}, M_{yz} *and* M_{zz}).

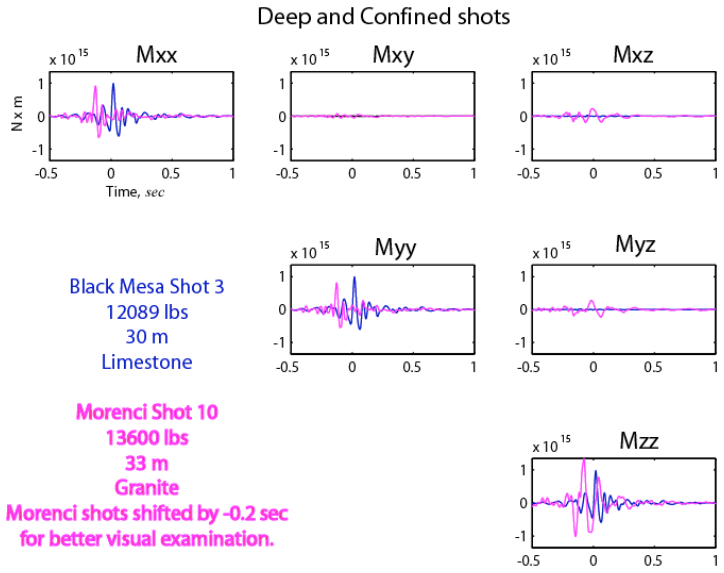

Figure 6. A comparison between the moment tensors for explosions in limestone at a coal mine (Black Mesa, shown in blue) and granite at a copper mine (Morenci, shown in magenta). From Zhou et al. (2005).

Figure 6 shows the moment tensor inversion results from previous explosion experiments. Both shots shown in Figure 6 are confined. One of the shots was carried out in a coal mine in limestone (Black Mesa), the other one was conducted in a copper mine in granites (Morenci). The diagonal elements of the moment tensor dominate. However, the relative size of the diagonal elements for the Black Mesa shot are almost the same, while for the Morenci shot the amplitude of M_{zz} components exceed the amplitudes of M_{xx} and M_{yy} components.

The inferred CLVD component could be either an artifact of an inadequate velocity model, or it could be explained by a non-point source from the cone of damage above a source. Unfortunately we had a very limited number of stations usable for the inversion. More research is needed on the influence of the noise on the moment tensor resolution.

CONCLUSIONS AND RECOMMENDATIONS

We continue to examine the differences in the moment tensors for chemical explosions in different media with variable confining conditions. In this article we used a frequency-domain linear inversion to find the time-dependent source moment tensors of five chemical explosions detonated during the New England Damage Experiment, conducted in Barre, VT in the summer of 2008. The goal of this experiment is to characterize the rock damage from an explosive source and to identify the source(s) of shear wave generation.

The Green's functions required for the moment tensor inversion were computed using *CPIS3.30* software (Herrmann, 2002). We developed a 1D Earth model for the test site based on the laboratory velocity measurements as well as seismic refraction travel time data. The moment tensor inversions have the dominant diagonal elements; however some explosions have significant off-diagonal components. The horizontal diagonal component (M_{xx} and M_{yy}) are similar in size, while the vertical M_{zz} is about twice as large as each of the horizontals. This may be a combination of either an isotropic and a CLVD sources, or an isotropic and a vertical force. The size of the isotropic component varies between 72 % and 79 % for different shots. The ratio of the isotropic component doesn't appear to correlate with the type of the explosives in our experiments, despite the differences in the shear waves generated by the different shot types (Leidig et al., [2009, these Proceedings]). The moment tensors from the previous experiments conducted in granites (Morenci copper mine, Zhou et al., 2005) are consistent with the results obtained in Barre granites. For future work, we will examine the moment tensors for the NPE for comparison to these results.

ACKNOWLEDGEMENTS

We wish to thank David Yang for his assistance on this project and for loaning us his code. We also wish to thank Peter Boyd for providing velocity information for the cores from NEDE.

REFERENCES

Ashby, M.F. and C. G. Sammis (1990). The damage mechanics of brittle solids in compressions, *Pure Appl. Geophys*. 133: 489–521.

Engelder, T., M. Sbar, and R. Kranz, (1977). A mechanism for strain relaxation of Barre Granite: opening of microfractures, *Pure Appl. Geoph*ys. 115: 27–40.

Feignier, B. and R. P. Young (1992). Moment tensor inversion of induced microseismic events: evidence of non-shear failures in the -4<M<-2 moment magnitude range, *Geophys. Res. Lett.* 19: 1503–1506.

Herrmann, R., H. (2002). An overview of synthetic seismogram computation. In *Computer Programs in Seismology, Version 3.30*.

Leidig, M., R. Martin, P. Boyd, J. Bonner, and A. Stroujkova (2009). Quantification of Rock Damage from Small Explosions and its Effect on Shear-Wave Generation: Phase I—Homogenous Crystalline Rock, these Proceedings.

Leidig, M., J. Bonner, J. Britton, K. Murphy, D. T. Reiter, J. Lewkowicz, S. Huffstetler, P. Boyd, R. Martin, D. Murray, A. Garceau, T. Rath, P. West, J. Trippiedi, M. McGinley, A. McGinley, W. Zamora, L. Foley, D. Richter, R. Garfield, A. Martinez, J. Reid., and R. Haas, (2008). Quicklook: Quantification of Rock Damage from Small Explosions and its Effect on Shear-Wave Generation, Weston Geophysical Corp. Report WG-QL0801, 77 p.

Patton, H., J. Bonner, and I. Gupta, (2005). *Rg* Excitation by Underground Explosions: Insights from Source Modeling the 1997 Kazahkstan Depth of Burial Experiments. *Geophys. J. Int.* doi:10.1111/j.1365-246X.2005.02752.x

Richter, D. A. (1987). Barre granite quarries, Barre, Vermont, in *Geological Society of America Field Guide – Northeastern Section*, 239–242.

Sammis, C. G. (2002). Generation of High-Frequency *P* and *S* Wave Energy by Rock Fracture During a Buried Explosion: Its Effect on *P/S* Discriminants at Low Magnitude, in *Proceedings of the 24th Seismic Research Review - Nuclear Explosion Monitoring: Innovation and Integration*, LA-UR-02-5048, Vol 1, pp. 542–551.

Stevens, J.L., G. E. Baker, H. Xu, T.J. Bennett, N. Rimer, and S.M. Day (2003a). The physical basis of *Lg* generation by explosion sources. in *Proceedings of the 25th Seismic Research Review - Nuclear Explosion Monitoring: Building the Knowledge Base*, LA-UR-03-6029, Vol. 1, pp. 456–465.

Stevens, J.L., N. Rimer, H. Xu, G.E. Baker, S.M. Day, (2003b). Near-field and regional modeling of explosions at the Degelen test site. SAIC Final Report SAIC-02/2050.

Stump, B., and L. Johnson (1977). The determination of source properties by the linear inversion of seismograms, *Bull. Seis. Soc. Am*. 67: 1489–1502.

Yang, X. (1997). Mining explosion and collapse source characterization and modeling with near-source seismic data. Ph.D. Thesis, Southern Methodist University, Dallas, Texas.

Yang, X. and J.L. Bonner (2009). Characteristics of chemical explosive sources from time-dependent moment tensors. *Bull. Seism. Soc. Am.* 99: 36–51.

Zhou, R., B. W. Stump and X. Yang (2005). Moment tensor inversions of single-fired mining explosions at a copper mine in Arizona, *Eos Trans. AGU*, 86(52), Fall Meet. Suppl., Abstract S11B-0166.